

UNIFIED MODEL DOCUMENTATION PAPER NO 45

THE THERMODYNAMIC / DYNAMIC SEA ICE MODEL

J F Crossley
D L Roberts

Version 1, Dated 2/10/95

(Valid for version 4.0 of the UM system.)

Modification Record

Document version	Author	Description.....

1. Introduction

Sea-ice plays a unique and important role in the global climate system. It not only interacts with both the ocean and the atmosphere, but interferes with direct communication between them. In attempting to simulate climate by developing global coupled atmosphere-ocean models, we are thus obliged to devote some attention to modelling sea-ice.

The presence of sea-ice has many consequences. Perhaps the most obvious of these is the change in surface albedo: ice-free ocean has an albedo of about 0.06 (except when the solar zenith angle is very high), but the albedo of snow-covered ice can easily exceed 0.8. There is thus the possibility of positive feedback between decreasing ice cover and increasing absorption of solar radiation at the surface; this 'ice-albedo feedback' is generally regarded as a potentially significant mechanism for amplifying climatic changes.

Sea-ice also constitutes a barrier to the direct exchange of sensible heat and moisture between the ocean and the atmosphere. As a simple example of the effect of thermal insulation, consider an (idealised) sheet of uniform sea-ice two metres thick. If the temperature of the top surface of the ice is -20°C , the conductive heat flux upwards through the ice will be roughly 20 Wm^{-2} : an order of magnitude less than the heat flux that would be lost by the ocean if ice were absent. A relatively thin covering of snow on the ice can make a significant further reduction in the heat loss.

Another important aspect of sea-ice is its influence on the salinity of the surface layers of the ocean. As sea-water freezes, most of its salt content does not become incorporated into the ice, but is instead discharged into the water below. Since the density of sea-water is an increasing function of salinity, this discharge of salt tends to destabilise the water column and thus enhances convection in the surface mixed layer. Conversely, the melting of ice deposits relatively fresh water at the surface and so reduces vertical mixing. Furthermore, in regions where the rate of ice production is high, the resulting cold saline water can be dense enough to sink to very deep levels, forming ocean bottom water.

The advection of sea-ice by winds and currents not only alters its geographical distribution, but also results in a transport of heat and salt. Ice tends to melt, on average, in lower latitudes than it forms. Since latent heat is released during freezing and absorbed during melting, there is consequently a net negative heat transport towards the equator. Similarly there is a negative equatorward salt transport, for the reasons explained in the previous paragraph. Most of the processes described above are represented in the sea-ice model to be described in this note, although in many cases the representation used is very simple with room for improvement. In the next section, a very brief review of sea-ice modelling is given, to provide a source of background information for the interested reader. This is followed in sections 3 and 4 by a description of the model as presently implemented.

2. Review

A full review of the large body of literature on sea-ice modelling will not be attempted here. However, it is worth considering some of the most influential papers. They may be divided into two broad categories: those that deal only with the thermodynamics of sea-ice, and those that also model ice dynamics.

A highly detailed treatment of sea-ice thermodynamics was set out by Maykut & Untersteiner (1971). Their one-dimensional model includes such refinements as the effect of internal heating due to the penetration of solar radiation, and the variation of thermal conductivity with depth due to non-uniform salinity. They also used a (vertical) resolution of 10 cm, which typically corresponds to 20 to 40 levels. Admirable though this work is, Maykut & Untersteiner's model is so complex that it is unsuitable for use in global climate studies, where there are many competing demands on the available computing resources. Semtner (1976) therefore produced two simplified thermodynamic models intended for use in large-scale simulations. One of these has three layers: two of ice and one of snow. The other is an even simpler version which became known, somewhat confusingly, as the zero-layer model, because though it provides for a layer of ice and a layer of snow, temperatures within the ice and snow are not computed. In a subsequent paper, Semtner (1984) compared the performance of his three-layer and zero-layer models with the Maykut & Untersteiner model, using boundary conditions characteristic of the central Arctic. He concluded that the price of the simplicity of the zero-layer model is some reduction in the accuracy with which the seasonal cycle of ice depth is simulated. The zero-layer model slightly overestimates the amplitude of the cycle and advances its phase by up to a month, so that melting begins in May instead of June, for example.

A model that includes a fairly sophisticated representation of the dynamics of ice, as well as thermodynamic effects, was devised by Hibler (1979). Hibler's model calculates the field of ice velocities from a momentum equation which includes the effects of wind and current stresses, Coriolis force, the internal ice stress, and the tilt of the sea surface. It is the treatment of the internal ice stress that introduces the greatest complications. Hibler chose to model sea-ice as a nonlinear viscous compressible fluid, with its viscosity dependent on the rate of deformation. The strength of the ice is also a function of its thickness and the compactness of the ice cover.

Attempts to model dynamical effects without the complexity and computational expense involved in Hibler's model have been made. For instance, Parkinson & Washington (1979) decided not to include the internal ice stresses explicitly, but to iteratively readjust the computed ice velocity field in such a way that ice was prevented from excessively converging into any grid box. This is probably the weakest aspect of an otherwise well-constructed model, notable for a detailed parametrization of the effects of leads. Hibler has produced a simplified version of his model, the so-called cavitating fluid model, which takes account of convergent stresses in the ice, but ignores the shear stresses, (Flato and Hibler 1990).

The representation of ice thermodynamics in the Unified Model is based on Semtner's 'zero layer' treatment, with a leads parameterisation based on that of Hibler (1979). This may be used as it stands, or one of two ice dynamics models may be included with it. The most widely used ice dynamics option is a very simple scheme based on Bryan (1969) in which ice depth, ice fraction and snow depth are advected using the surface level currents calculated by the ocean model. The inclusion of this scheme has allowed flux correction of ice depth to be dispensed with in coupled climate runs.

The other ice dynamics option available within the UM is based on Hibler's simplified model, the "cavitating fluid" scheme, which neglects shear stress. This option is computationally more expensive and has not been shown to give significantly better results than the crude advection scheme at climate resolution.

3. Description of Thermodynamic Model

The basic purpose of a thermodynamic sea ice model is to ensure that the net heat fluxes from atmosphere and ocean into the ice, snow and leads are balanced by changes in ice and snow mass. It is important to make clear at the outset that the sea-ice model implemented in our system is split into two parts. One part resides within the atmospheric model and deals with the interactions between sea-ice and the atmosphere. The other part resides within the ocean model and deals with the interactions between sea-ice and the ocean, as well updating the primary ice model variables. There are good reasons for this division, which was originally suggested by Gordon & Bottomley (1984). On one hand, it allows the surface temperature of the ice/snow system to interact fully with the diurnal cycle of radiation. On the other hand, it allows changes in ice depth and concentration to be carried out inside the ocean model, which reduces the problems that arise when the status of a grid box (icy or ice-free) changes part of the way through a coupling interval. A fuller discussion can be found in the document by Gordon & Bottomley (1984) (although to avoid confusion it should be mentioned that Gordon & Bottomley anticipated updating the ice variables only once per coupling interval, whereas in the eventual implementation the ice variables are updated with the same frequency as the ocean model temperatures and salinities).

Interactions between the sea-ice model and the atmospheric model thus consist largely of the former providing a lower boundary condition (with variable surface temperature) for the latter, which supplies in return various forcing fluxes that are accumulated during the atmospheric phase and used to update the ice model during the ocean phase. The way in which the surface fluxes of long- and short-wave radiation are calculated for grid boxes containing sea-ice is described in documentation paper 23 by Ingram (1990), so a detailed description will not be repeated here. However, as the specification of the surface albedo of sea-ice can have a very important effect on the simulation of the ice, the albedo formulation will be explained. The albedo of the sea-ice fraction of the grid box, α , is specified as a simple function of the surface temperature of the ice, T , by fixing $\alpha = \alpha_c = 0.8$ at and below $T = -10^\circ\text{C}$, $\alpha = \alpha_m = 0.5$ at $T = 0^\circ\text{C}$, and varying α linearly with temperature between these two points. The values α_c and α_m , and the temperature range over which the albedo varies, are specified through the user interface as parameters to atmospheric physics section 1, Shortwave Radiation. This variation of albedo with surface temperature has been used as a method of tuning the thermodynamic ice model, but care is needed because increasing the albedo increases the ice-albedo feedback and can make the model too sensitive to, for example, changing cloud cover. The albedo of the leads (open water) fraction of the grid box is taken to be the same as that of open sea, 0.06. A grid box mean surface albedo is then calculated from the albedos of the ice and leads portions of the box, by weighting them with the fractional areas covered by ice and leads respectively, and this is used in computing the effect of multiple reflections between the snow/ice surface and the base of clouds visible from the surface. Note, however, that the net downward surface flux of short-wave radiation is computed separately for the ice and leads portions of a grid box, as indeed is the case for long-wave radiation. The albedo calculations are carried out within the atmosphere model in subroutine FTSA.

One or two comments should be added before leaving the subject of surface albedo. First, the temperature variation is intended to represent such processes as the ageing of any snow cover and the formation of melt ponds, as the surface temperature nears melting point. Note that the model deals with the mean surface temperature of all the ice floes in a grid box, and sub-gridscale variations will result in some locations having temperatures slightly above or below the mean value. Thus it is appropriate

to spread the albedo changes over a small range of temperatures. Secondly, it may seem strange that the upper limit of this temperature range should be the freezing point of fresh water rather than that of sea-water (-1.8°C). It turns out that 0°C is a better choice for two reasons: any snow that falls on the ice is of course non saline, and the salt content of the ice itself gradually percolates downwards, so that with the exception of floes less than a year old, the upper surface of the ice is also low in salt. A freezing point of 0°C is also used in the atmospheric boundary layer subroutines. Finally it should be clearly stated that the present albedo formulation is simplistic. No account is taken of the thickness of the ice, the depth of the snow cover, or the increase in (spectrally-averaged) albedo under overcast skies. The importance of these and other effects is discussed in a paper by Shine & Henderson-Sellers (1985), which would be a good starting point for future work on improving the albedo formulation. A proposal for a spectrally-dependent surface albedo scheme for sea ice has been written by D.Roberts in Hadley Centre internal note No. 35. (D. Roberts 1993)

As well as radiative fluxes, the atmosphere model must supply the sea-ice model with the turbulent fluxes of latent and sensible heat. Again, these fluxes are calculated separately for the portions of a grid box covered by ice and leads, with the appropriate Richardson number used to characterise the stability of the surface layer in each case. Note that the surface temperature of the leads is assumed to be T_F , the freezing point of sea-water, for all purposes. This assumption may not be entirely appropriate in the marginal ice zone, particularly in experiments which include ice dynamics, as the top level ocean temperature can be significantly above freezing in a grid square which includes the ice edge. There is good observational evidence that the presence of even a small fractional coverage of leads can increase the grid box average fluxes of heat and moisture substantially. See, for example, the lidar data reported by Barry & Miles (1988). Full details of the model's boundary layer formulation over ice and leads are given in documentation paper 24 by Smith (1990).

We now turn to the ice model itself. This is based on the 'zero-layer' thermodynamic model of Semtner (1976), in which the prognostic variables are surface temperature T , ice depth h_I , and snow depth h_s . Temperatures within the ice and snow are not computed; the internal temperature field is assumed to be piecewise linear (but see below), with a change of gradient at the ice/snow interface because of the lower thermal conductivity of snow. Thus the atmospheric half of the model uses an 'equivalent ice depth' h_E , defined by

$$h_E = h_I + \kappa h_s \quad (3.1)$$

where $\kappa = \kappa_I/\kappa_s$ is the ratio of the thermal conductivities of ice and snow. The downward diffusive heat flux through the ice and snow is then F_D , where

$$F_D = \kappa \frac{(T - T_F)}{h_E} \quad (3.2)$$

This equation uses the fact that the temperature of the lower surface of the ice must be T_F , since this is the temperature at which ice and sea-water can coexist in equilibrium. At present, T_F is taken to be a constant, -1.8°C . However this is only a convenient approximation; T_F is actually a function of salinity and pressure. While the pressure effect is negligible, except beneath the ice shelves of the Antarctic, the salinity dependence should not be dismissed altogether, and may be worth including in future versions of the model.

The prognostic equation for T is

$$c_* \frac{dT}{dt} = F_A - F_D \quad (3.3)$$

where F_A is the net downward atmospheric heat flux at the surface of the ice (or snow, if present), and c_* is an effective surface heat capacity. The surface heat capacity term was not part of Semtner's zero-layer model, which neglects heat storage by the ice and assumes a linear temperature profile, as has already been noted. This term was introduced by Gordon & Bottomley (1984) in order to improve the simulation of the diurnal cycle of surface temperature. The constant c_* is assigned a value corresponding to the heat capacity of a depth of ice proportional to the e-folding depth of the diurnal temperature wave (about 20cm, giving $1/c_*=4.8e-6$). Provided that this depth is much less than h_E , this procedure is satisfactory. In the code, the reciprocal of c_* is stored in comdeck C_SICEHC to avoid unnecessary divisions, and equation (3.3) can be found in the boundary layer subroutine IMPL_CAL. The calculation of F_D occurs in subroutine SICE_HTF. As pointed out by Gordon & Bottomley (1984), for thin ice floes the surface heat capacity should be made to depend on the actual ice depth, but this complication has not been included in the current version of the model. The inclusion of this heat storage term can introduce some inconsistencies into the coupling of atmosphere and ocean models. Since the ice or snow surface temperature is not communicated to the ocean part of the ice model, where ice melts completely, through basal melting, it is possible for the heat required to raise the ice surface temperature to 0°C to be neglected. In practice, if the ice is about to disappear its surface temperature is likely to be at, or close to, the melting point so any heat source or sink will be negligibly small. (Locally it can be of order 0.1 W.m⁻² but the global, annual total is mW. J.Gregory pers.comm.)

One subtlety that was glossed over in the previous paragraph is that, according to Gordon & Bottomley (1984), the F_D term in equation (3.3) should be evaluated not with the instantaneous value of T , but with a surface temperature averaged over a time interval of at least a day. This is because the linear temperature profile assumed by Semtner's model is not applicable to the diurnal timescale. However, in practice the scheme has never been implemented in this way: F_D has always been computed with the instantaneous value of T . It would be quite feasible to follow the approach originally intended by Gordon & Bottomley (1984), by computing F_D during the ocean part of the model. This would require the diurnal mean of T to be passed from the atmosphere to the ocean model, and F_D to be passed from the ocean to the atmosphere model. Whether this would significantly improve the simulation is an open question.

As explained at the beginning of this section, the atmospheric part of the model deals with the surface temperature of the ice/snow, while the ocean part of the model updates the ice depth and concentration. Thus equations (3.2) and (3.3) belong to the atmospheric part of the model. (In fact they are present even when the atmospheric model is run in uncoupled mode, with ice depths and concentrations specified from climatology.) The way in which the two parts of the model communicate must now be considered.

During an atmospheric phase, F_D is calculated using (3.2). The time-average value of this diffusive heat flux is passed to the ocean model, where it is to be used to control the ablation or accretion of ice at the interface between the ice and sea-water. Another heat flux is also diagnosed during the atmospheric phase. This is the surface melting heat flux F_M , which is zero as long as the surface of the ice or snow remains below melting point, taken to be 0°C for the reasons explained earlier when describing the albedo calculation. If T attempts to rise above melting point, the atmospheric model code in subroutine SF_EVAP resets it to melting point and stores the corresponding positive heat flux implied by

the temperature change in F_M . Thus if T_z is the (fictitious) intermediate surface temperature (in Celsius), F_M is given by

$$F_M = \frac{C_* T_z}{\Delta t} \quad (3.4)$$

where Δt is the length of the timestep. The time-averaged value of F_M is also passed to the ocean model, where it is used to control melting at the upper surface of the ice floe.

In addition to the fluxes F_M and F_D , (which are called TOPMELT and BOTMELT in the ocean model), the atmospheric model also supplies the ocean model with the rates of snowfall and sublimation. Whereas the snow depth at land points is updated within the atmospheric model, the snow depth at sea-ice points is updated within the ocean part of the ice model. Thus the time-averaged rates of snowfall and sublimation are required. Of course, in the absence of snow cover sublimation reduces the ice depth instead. The time-averaged values of the net atmospheric surface flux over the leads portion of sea-ice grid boxes, split into its non-penetrative and penetrative components, are also made available to the ocean part of the ice model. The "penetrative" component is all solar radiation in most ocean-only experiments, but in the coupled model is defined as only Band I of the four solar radiation bands (which contains the visible and near IR part of the spectrum). The "non-penetrative" component is the sum of net sensible and latent heat fluxes, and longwave radiative fluxes between ocean and atmosphere. In the coupled model this includes bands II-IV of the shortwave radiation. All these heat fluxes are combined because they are absorbed within the top few centimetres of the ocean, the "penetrative" flux being the exception. In practice, the fluxes are stored in the same arrays as those used for the non-penetrative and penetrative surface fluxes at ice-free ocean points (known as HTN and SOL respectively in the ocean model). This has the advantage that if the status of the grid box changes from icy to ice-free during an ocean phase, the ocean automatically receives reasonable surface heat fluxes until the next atmospheric phase. Conversely, if a grid box begins to freeze part of the way through an ocean phase, sensibly-defined leads fluxes will be used. The fluxes are also weighted by the ice-free proportion of the grid box, giving grid box mean fluxes. This allows heat to be conserved despite changes in the ice concentration during ocean phases. Note that the sublimation rate and the fluxes F_M and F_D are weighted by the ice concentration for the same reason. As an aside, the wind mixing energy field, which is required as input to the mixed layer model, is treated differently by the atmosphere model at ocean and ice points. A special "leads" value of wind mixing energy, calculated using the drag coefficient appropriate for leads rather than the grid box mean, is supplied to the ocean at ice points. This is done because the grid box mean value gave unrealistically deep mixed layers under ice. Climatological values of wind mixing energy are not usually available at ice points for ocean only experiments.

It is probably useful to pause here and discuss the ice model's requirements in ocean-only simulations. The above discussion of atmospheric fluxes applies to the coupled model. In experiments with the ocean model, all surface fluxes are supplied as ancillary files with the data taken either from observational climatologies or from previous experiments with the atmosphere or coupled model. There are two ways of providing the ice model with these surface fluxes. In experiments to spin up the ocean, such as climate change experiments, it is often desirable for the ocean-only stage to be as similar as possible to the coupled experiments that follow it. To do this, surface fluxes from a coupled experiment are often averaged to provide an annual cycle of 5 day mean forcing fields, which are then applied throughout the ocean experiment.

In an experiment like this, the ice model would require those fields which the atmosphere supplies in a coupled experiment, namely F_M (or TOPMELT), F_D (or BOTMELT), snowfall, sublimation, and the penetrative and non-penetrative leads fluxes (SOL and HTN). In fact the ocean model will require the leads fluxes in any case. One drawback with this type of forcing is that the fluxes are fixed and therefore do not respond to changes in ice depth and extent during the ocean experiment. For example, F_D is inversely proportional to the ice depth so it can be quite large for thin ice, but thicker ice tends to lose less heat. If F_D is diagnosed in an experiment with thin ice at a particular location, but the ice subsequently thickens in the spin up phase, the large heat loss appropriate for thin ice will continue to be applied and runaway ice growth could result. In practise this effect would be masked by relaxation of the ice depth towards climatology in many experiments, but it can make sensitivity experiments hard to interpret.

Another option for supplying the ice model with surface fluxes is available, in which F_D , F_M and the non-penetrative leads flux to be used by the ice model are calculated in subroutine PSEUDAIR. The calculations use total downward solar radiation and surface air temperature (1.5 m temperature) as inputs, so these two fields must be provided as ancillary fields, replacing F_D and F_M . The Schutz and Gates air temperature climatology includes values at sea ice points, and zonal mean solar radiation from the 3rd annual cycle (which had specified cloud) has been used. Snowfall and sublimation may also be supplied from ancillary files, but if climatological values are not available, fields of zeroes may be included in the initial dump for these fields. This option avoids the problem with changing ice depth described above, since the surface fluxes are calculated within the ice model with changing ice depth and fraction allowed for, but the subroutine used to calculate the fluxes is rather crude, and would benefit from some model development work. A logical switch in the user interface controls which type of surface forcing is used in ocean only experiments. In addition to the above fields, if the ice depth is to be relaxed towards climatology (which is usually done only if ice dynamics is not included), it is necessary to provide an ice depth climatology, and it can be helpful if this is consistent with the climatological SST field. (Note that at present this subroutine calculates net solar radiation into leads, but this field is not used because it is now usually applied within the ocean model. Since the climatological values of net solar radiation, obtained from ancillary files, are likely to be zero or missing data at sea ice points, it may be sensible to move the calculation of this and the non-penetrative surface flux from ICE_CTL to INIT_OCEAN_ICE and pass these values to the ocean model at sea ice points.)

Within the ocean model, the net surface fluxes over ocean or leads are treated in a way which can be very confusing. I shall begin by describing what happens in coupled models which include one of the ice model options (except the "pseudo ice" model, which is discussed fully in Appendix B). In all types of ice model, the penetrative surface flux through leads/ocean (SOL) is used by the penetrative solar radiation code in the ocean model as it is at ice free points. The only difference is that the net flux will be smaller (because it was calculated only for the leads fraction of the grid box). If the "thermodynamics only" version of the sea ice model is selected, all the non-penetrative surface leads/ocean flux (HTN) is used by the ice model to form or melt ice. In this case HTN does not affect ocean model temperatures at ice-covered points. If either of the ice model versions with ice dynamics are chosen, the non-penetrative surface flux is split (in subroutine INIT_OCEAN_ICE) at grid points where ice has formed so that part of it affects ocean temperatures, and the rest is used to melt or form ice. This split is done, rather arbitrarily, using the ice fraction A , so that $A*HTN$ is used in the ice model and $(1-A)*HTN$ warms or cools the ocean. The splitting prevents excessive ice formation where small amounts

of ice advect over a strongly cooling ocean. Ocean-only models which supply coupled model like forcing for the ice model (as described earlier) treat these two fluxes in exactly the same way, since they are assumed to have been diagnosed in a coupled model. In ocean-only models which derive the sea ice and leads fluxes from 1.5m temperature and downward solar radiation, there are some subtle differences. As in coupled models, the penetrative surface flux in leads is always applied to the ocean, and the non-penetrative flux is split between ice and ocean if ice dynamics is included, and used entirely to melt or form ice in thermodynamics-only models. However, it is assumed that the climatological values of surface fluxes supplied from ancillary fields (SOL and HTN) are valid only over open ocean grid squares or the leads fraction of an ice-covered grid square, i.e. that they have not been weighted at sea ice points by the leads fraction to give a grid box mean flux as would occur in the atmosphere model. For this reason the two surface fluxes (SOL and HTN) are weighted by the leads fraction at sea ice points. The weighting occurs in INIT_OCEAN_ICE for HTN and in FLXBLANK (called from TRACER) for SOL.

We now move on, to consider the ocean half of the thermodynamic ice model. The general sequence of events is that first the snow depth h_s is updated, followed by the ice depth h , and then the ice concentration A . One slightly anomalous feature of the formulation is that the model works with the ice depth averaged over the whole grid box, h , whereas the variables introduced earlier, h_i and h_s , are the ice and snow depths averaged over the ice-covered portion of the grid box alone. Thus h and h_i are related by:

$$h = Ah_i \quad (3.5)$$

Let the rates of snowfall and sublimation be S_N and S_B respectively. (Their units are kilogram per square metre per second.) Then the equation for h_s is:

$$\rho_s \frac{dh_s}{\Delta t} = S_N - S_B - \frac{F_M}{L} \quad (3.6)$$

where ρ_s is the density of snow and L is the latent heat of freezing of water. In practice, the snow depth is updated in two stages, first by the snowfall and sublimation terms and secondly by the F_M term. After each stage there is a check to see whether h_s has dropped below zero. If so, it is reset to zero, and any surplus energy implied to be left over is put aside for input to the ice depth equation. The two stage process enables excess sublimation and excess F_M to be kept track of separately, which is necessary because the implied effect on ocean salinity differs in the two cases. For present purposes the corresponding combined surplus heat flux from these terms will be denoted by X .

The ice depth equation is complicated by the need to take account of the change in ice depth due to the net surface heat flux into the leads fraction of the grid box, F_L . This is made up of net shortwave and longwave radiation (only Bands II-IV of the shortwave), sensible and latent heat fluxes, which have been combined into the nonpenetrative surface (HTN or HEATFLUX), and weighted as described above. Thus F_L is the net non-penetrative surface heat flux for leads in the sea ice heat budget (i.e. not including the part which affects ocean temperatures). Writing the prognostic equation for the grid box mean ice depth as

$$\frac{dh}{\Delta t} = AR_i + (1-A)R_L \quad (3.7)$$

where R_i and R_L are the rates of change of h due to net fluxes over the ice and leads respectively, we have:

$$L \rho_I R_I = -F_B - F_D - X - C \quad (3.8)$$

$$L \rho_I R_L = -F_L - F_B + LS_N - C \quad (3.9)$$

In these equations, ρ_I is the density of ice and F_B is the heat flux from the top layer of the ocean into the ice, to be discussed later. The term C is a latent heat flux, which is generated by resetting ocean surface temperatures which fall below freezing point to T_F during the ocean model part of the integration, and storing the implied heat flux in array CARYHEAT for use by the ice model. If the ocean surface temperature falls below T_F at a point with no sea ice, ice formation is triggered. (This is done in subroutine FREEZEUP, which also takes care of unrealistic temperatures, at any level of the ocean, that may have been produced by advection or isopycnal diffusion by mixing the heat down. A similar exercise is carried out in subroutine REFREEZE, after Fourier filtering the ocean temperature field, but filtering is not allowed to trigger ice formation.)

The heat flux from the ocean into the ice, F_B , is assumed to be related linearly to the difference between the temperature at the base of the ice and the temperature of the top layer of the ocean, T_1 . Thus

$$F_B = K \rho_w c_p \frac{(T_1 - T_F)}{(0.5 d)} \quad (3.10)$$

where ρ_w is the density of seawater, c_p is its specific heat capacity, and d is the thickness of the first ocean layer. Here K is an 'eddy diffusion coefficient' (in $\text{m}\cdot\text{s}^{-1}$) which is effectively a tunable parameter, chosen through the user interface (the HADCM2 transient experiments used a value of $2.5\text{e-}5 \text{ W}\cdot\text{m}^{-2}\cdot\text{K}^{-1}$). Increasing K increases the positive heat flux from ocean to ice per degree temperature difference. Note the dependence of F_B on the depth of the first ocean level, which means this parameter requires alteration if the vertical resolution is changed (for example in the slab model, with a 50m mixed layer). This parameterisation of F_B has been used before, for example by Pease (1975). It was criticised on several grounds by Parkinson & Washington (1979), but is perhaps the best that can be done without implementing a proper boundary layer scheme. For observational estimates of F_B , see MacPhee (1992) and Omstedt and Wettlaufer (1992). Incidentally, F_B has been included in the contribution to the net flux for the leads portion of a grid box (3.10), because there seems to be no obvious physical reason why there should not be an upward heat flux in the entire surface layer of the ocean, instead of only beneath the ice-covered portion. Recent experiments with the version of the model which includes ice advection suggest that in future it may improve the simulation if this point, and the treatment of fluxes in leads and at the ice edge generally, are reconsidered.

Changes in the ice concentration associated with thermodynamic processes are modelled using a formulation that Hibler (1979) used in his combined dynamic-thermodynamic model. The assumptions underlying this formulation are discussed at length in Hibler's paper. They lead to the following equation:

$$\frac{dA}{\Delta t} = (1-A) \frac{R_L H(R_L)}{h_0} + \left(\frac{A}{2h}\right) \frac{dh}{\Delta t} H\left(\frac{-dh}{\Delta t}\right) \quad (3.11)$$

where H is the Heaviside function, defined to be zero when its argument is

negative, and one when its argument is positive. The parameter h_0 can be thought of as representing the minimum depth to which newly-formed ice must grow before it is counted as belonging to the ice-covered fraction of the grid box. Following Hibler's recommendation, this parameter has been assigned a value of 0.5m. Before leaving (3.11), it should be mentioned that M Bottomley & C Gordon (personal communication) and also O S Lee (personal communication) have independently discovered that (3.11) is not, in fact, entirely consistent with the assumptions made by Hibler (1979). The second term in (3.11), which represents the opening up of leads when the ice is melting, is inaccurate when the ice is close to disappearing altogether. At present it is considered that this defect in the scheme is not important enough to warrant correction.

Since completely unbroken ice cover is very rarely encountered in reality, because of small-scale deformations of the ice pack, A is prevented from exceeding an upper limit, currently set to be 0.995 in the Northern Hemisphere and 0.98 in the Southern Hemisphere. This practice was adopted by Parkinson & Washington (1979); the limits are somewhat arbitrary but reflect observational evidence that Antarctic ice tends to be less compact. In addition, as long as h remains non-zero A is prevented from dropping below a lower limit, currently set to 0.001. This device is intended to avoid the risk of numerical problems associated with very small values of A . As another safety measure to prevent numerical problems in the atmosphere model, h itself is never allowed to become smaller than 0.0001m. Any smaller amounts of ice are melted, with the latent heat required to do this borrowed from the ocean.

The snow depth h_s was defined earlier to be averaged over the ice-covered part of the grid box only. It is assumed that the snow cover is in fact uniformly distributed over the ice floes in a grid box. This means that changes in A imply further changes in h_s . If A has increased, the model redistributes the existing mass of snow over the wider area of ice in the grid box. On the other hand, if A has decreased, the snow on the portion of ice that melted is treated as falling into (and cooling) the leads, so that h_s is left unchanged.

It is worth mentioning here that although F_b is the major heat flux from the upper ocean into the ice, heat flux C (obtained by resetting sea surface temperatures to T_F) and the various additional bits of heat used by the ice model, such as the latent heat of melting snow mentioned above, also transfer heat from ocean to ice and vice versa. All these additional heat fluxes are combined and stored in an array called CARYHEAT which is held in the dump. Within each ocean timestep, first all the ocean calculations are completed, including the addition of heat flux C to the ocean and its storage in CARYHEAT. After this the ice model calculations are carried out, and C is included in the ice and snow heat budget so array CARYHEAT is no longer required to store it. The ice model also diagnoses the additional little heat fluxes such as melting snow in leads and requires to communicate these with the ocean model on the next timestep. In order to save space, the same array CARYHEAT is used to store this heat flux in the dump for use by the ocean on the next timestep. Because of this double use, if an accurate heat budget calculation is to be done CARYHEAT must be diagnosed twice. Heat flux C is available as a section 30 diagnostic, and the miscellaneous heat flux from the ice model is available as a section 0 ocean prognostic variable. Neither of these fluxes is likely to be much larger than 1 Wm^{-2} in the present model formulation, but they can cause a great deal of confusion.

Early versions of the model (as run on the Cyber) exhibited a tendency to produce unrealistically large accumulations of snow in some areas. A further modification to h_s is therefore made, to represent the formation of so-called 'white' ice. This is ice that forms at the snow/ice interface

when snow accumulates to such an extent that it depresses the ice below the waterline, observed in particular in Antarctic pack ice. Water then infiltrates the snow and tends to freeze there, forming 'white' ice. Ledley (1985) pointed out that this process is important because it restricts the thickness that the snow layer can attain, and therefore its ability to insulate the ice layer from atmospheric cooling. Using the hydrostatic equation, one can show that if w is the height of the waterline above the bottom of the ice, and ρ_w is the density of water, then:

$$\rho_w w = \rho_I h_I + \rho_S h_S \quad (3.12)$$

If w , as given by this equation, exceeds h_I , then the model turns a depth $(w-h_I)$ of snow into ice. A.Keen and W.Ingram (personal communication) found a small error in the way this has been implemented in the present model, which has not yet been corrected (although it is implemented correctly in the slab model).

One important topic that has not yet been addressed in this section is the impact of changes in the ice and snow depths on the salinity of the ocean surface layer. In representing this effect, the salinity of ice, S_I , is taken to be uniform. This is quite unrealistic, but justified in view of the complications that would be involved in keeping track of the history of the ice. The value assigned to S_I is at present 0.006; snow, on the other hand, has zero salinity. When sea-water freezes, not all the salt content of the water is incorporated into the resulting ice. If the salinity of the top layer of the ocean is S (typically in the range 0.030-0.035), the salinity increment ΔS associated with a change Δh in ice depth is given by:

$$\Delta S = \rho_I \Delta h \frac{(S-S_I)}{\rho_w d} + C_{SB} \quad (3.13)$$

where C_{SB} is a correction to allow for sublimation, to be discussed later. Now a curious assumption has been made in deriving this equation, namely that the mass of liquid water in the top ocean model grid box is independent of changes in the volume of ice. In order to understand why this assumption was made, it is helpful to consider the alternative. Suppose that when part of the water in the surface grid box froze, the mass of ice thus formed was deducted from the mass of liquid water in the box. In order to be consistent, all ocean model code that dealt with exchanges of momentum, heat and salt with or among surface layer grid boxes would need to be amended. The trouble caused by doing this would almost certainly outweigh any benefit gained.

The correction term in equation (3.13) arises because a reduction in ice depth due to sublimation does not liberate relatively fresh liquid water to reduce the salinity of the ocean, as would be the case if the ice had melted. Indeed, in order to conserve salt it is actually necessary to increase salinity to take account of the small salt content of the sublimed ice. The correction term can be shown to be:

$$C_{SB} = \left(\frac{S_B A S \Delta t}{\rho_w d} \right) H(S_B) \quad (3.14)$$

In this equation the sublimation rate S_B should, of course, be interpreted as the excess sublimation after any snow has been disposed of (cf the discussion following equation (3.6)). Furthermore, the Heaviside function is a reminder that any negative sublimation (i.e. deposition of frost)

increases the snow depth and has no effect on salinity.

The salinity increment resulting from melting snow (see equation (3.6)) is given by

$$\Delta S = - \left(\frac{A S F_M \Delta t}{L \rho_w d} \right) \quad (3.15)$$

where Δt is the timestep and the weighting factor A appears because h_s applies only to the ice-covered part of the grid box, unlike h . Note that the snowfall and sublimation increments to h_s do not directly affect the salinity (though they do so indirectly, by altering the amount of snow available for later melting). In addition, the model takes account of the salinity changes due to snow falling into leads and the conversion of snow to 'white' ice. In the conversion of snow to 'white' ice, a depth $(w - h_I)$ of snow is converted, where w is as defined in equation 3.12. This implies a salinity increment of

$$\Delta S = \frac{-A \rho_s (w - h_I) S_I}{\rho_w d} \quad (3.16)$$

due to 'white' ice formation. Where the fractional area of snow-covered ice has decreased by amount ΔA , an amount of snow $h_s \Delta A \rho_s$ is assumed to fall into the leads and melt. A salinity increment of

$$\Delta S = \frac{h_s \Delta A \rho_s S}{\rho_w d} \quad (3.17)$$

where ΔA is less than zero, is therefore added to the ocean on the next time step. The salinity increment calculated by the ice model is stored in array CARYSALT and added to the ocean top level on the next timestep by subroutine ICEFLUX.

It is now necessary to discuss the discretisation in time of the ice model equations. At first sight this appears to be simple; a forward timestep equal to the ocean model tracer timestep. Unfortunately matters are far from simple! The problem is that the ocean model uses a leapfrog timestepping scheme in which the values of temperature, salinity, currents etc are stored at two time levels, say levels $n-1$ and n . The new values at time level $n+1$ are generated by adding increments over a timestep of length $2\Delta t$ to the old values at time level $n-1$. This contrasts with the ice model, in which values at time level $n+1$ are generated by adding increments over a timestep of length Δt to the values at time level n . As a further complication, the ocean model occasionally makes a forward timestep, for instance on the first step after restarting from a dump. It does this by copying the time level n data to time level $n-1$, and multiplying fluxes etc by Δt instead of $2\Delta t$. The result of all this is that it is easy to become confused when thinking about the detailed interactions between the ice and

ocean models, but in practise energy conservation can be maintained by passing heat fluxes between the two and multiplying by the appropriate timestep in each model. This results in slight non-conservation on the ocean forward timesteps, but an attempt to correct this involved extra variables stored in the dump and resulted in an unstable ocean simulation with split solutions so was abandoned.

4. The Dynamic Sea Ice Models

Sea ice models which represent only thermodynamic processes have many shortcomings but have often been used in climate models because including a realistic parametrisation of ice dynamics can be computationally very expensive. The thermodynamic sea ice model which has been used by the Met. Office does not simulate the large annual range of southern hemisphere sea ice extent very well. The arctic extents can be made quite realistic with careful tuning and flux correction, but the thickness distribution is affected in the climate system by ice-ocean dynamics in the Arctic Basin, and this is not simulated by the model. The thermodynamic model has also shown itself to be relatively unstable when the flux correction fluxes, which are required to prevent climate drift, are used. Two ice model versions which incorporate ice dynamics are now available within the unified model system. The simplest, which has been used in the HADCM2 suite of transient climate change experiments, is a crude advection scheme based on that used at GFDL (Bryan 1960ish). The other is the cavitating fluid scheme of Flato and Hibler (1990 & 1992), which is computationally much more expensive and does not show an improvement in performance commensurate with this cost. The cavitating fluid scheme (which is used by the FOAM forecast suite 28/9/95) is described in Appendix C. The simpler scheme, which uses the same advection, is described below.

The simple advection scheme for sea ice diagnoses the total surface current from TRACER, and uses this to advect ice thickness, ice concentration, and snow depth. In order to avoid duplication of code, the upwind advection scheme used is that developed for the cavitating fluid ice dynamics scheme, on an Arakawa C grid. The total current is interpolated from the ocean B grid to the C grid, and ice depth is also interpolated to the C grid velocity points. If ice thicker than 4.0m (on the C grid) would be advected up the thickness gradient, the current component at that point on the C grid is zeroed. This is done as a crude parameterisation of the greater resistance of thick ice to convergence. The advective change in ice depth, part of the continuity equation, is given by

$$\frac{\partial h}{\partial t} = -\nabla \cdot (\mathbf{u}h)$$

where h is the mean ice depth. Similar equations hold for ice concentration, A , and grid box mean snow depth ($A.h_s$). The layout of the C grid used is shown in Figure 1 below. For each face of the grid square surrounding an ice depth point, a test is carried out on the sign of the velocity and the advective increment to ice depth determined as follows:

Face 1

$$\Delta h(u(i, j)) = u(i, j)h(i, j+1) \quad \text{length1/area} \Delta t \quad \text{if } u(i, j) \geq 0$$

$$\Delta h(u(i, j)) = u(i, j)h(i+1, j+1) \quad \text{length1/area} \Delta t \quad \text{if } u(i, j) < 0$$

Face 2

$$\Delta h(v(i, j)) = v(i, j)h(i+1, j) \quad \text{length2/area} \Delta t \quad \text{if } v(i, j) \geq 0$$

$$\Delta h(v(i, j)) = v(i, j)h(i+1, j+1) \quad \text{length2/area} \Delta t \quad \text{if } v(i, j) < 0$$

Face 3

$$\Delta h(u(i+1, j)) = u(i+1, j)h(i+1, j+1) \quad \text{length3/area} \Delta t \quad \text{if } u(i+1, j) \geq 0$$

$$\Delta h(u(i+1, j)) = u(i+1, j)h(i+2, j+1) \quad \text{length3/area} \Delta t \quad \text{if } u(i+1, j) < 0$$

Face 4

$$\Delta h(v(i, j+1)) = v(i, j+1)h(i+1, j+1) \quad \text{length4/area} \Delta t \quad \text{if } v(i, j+1) \geq 0$$

$$\Delta h(v(i, j+1)) = v(i, j+1)h(i+1, j+2) \quad \text{length4/area} \Delta t \quad \text{if } v(i, j+1) < 0$$

where Δt is the timestep. Lengths 1 to 4 are the lengths of the faces round each grid square, calculated using spherical geometry. Land points are masked. Similar calculations are done for ice concentration, and the product of ice concentration and snow depth, which will not be repeated here.

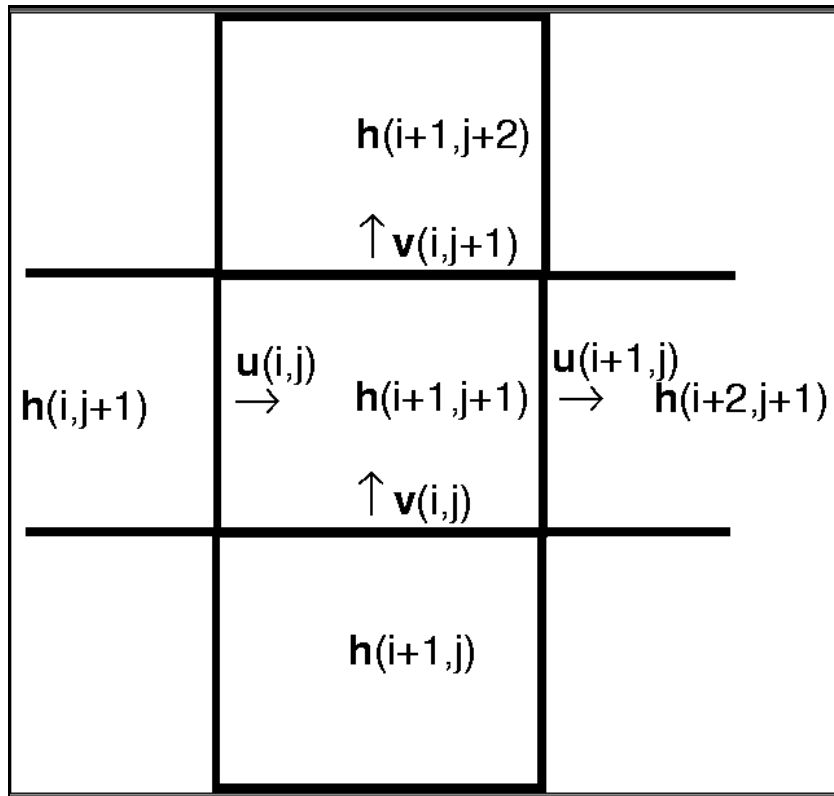


Figure 1 C grid velocities and ice depths

After the advective increments have been calculated and added (in subroutine ICE_ADVECT), del2 diffusion is applied to ice depth (only in the simple ice advection scheme). The diffusion coefficient is supplied through the user interface and a value of $2000. \text{m}^2\text{s}^{-1}$ was used in HADCM2. Since the upwind advection scheme used is itself very diffusive it may be worth reducing or removing the del2 diffusion of ice depth when an opportunity arises. The diffusion code is almost identical to that used in ocean subroutine TRACER, which is described in the Cox model documentation. The only significant difference within the ice model is that the land sea mask is extended to include open ocean grid points before diffusion increments are calculated. This prevents diffusion extending the ice edge, although advection is permitted to do so.

The ice dynamics routines are called immediately before the thermodynamic subroutine ICEFLOE updates the ice depth etc. Advection changes the ice thickness and fraction, and snow depth which are passed to ICEFLOE (also the logical array ICY which depends on ice fraction). If more than the minimum ice depth is advected into a previously ice-free grid square, and thermodynamic ice was about to form, the ice formation logical NEWICE is set to false, and the grid square is treated by the thermodynamics as one where ice already exists.

Appendix A: The Pseudo-Ice Model

For ocean-only integrations in which a full ice model is not required, the 'pseudo-ice' model may be used. The object of this code is to mimic the effect of sea ice on the surface boundary conditions of the ocean, without explicitly modelling the ice. The model consists of the following steps, performed at each tracer timestep:

i. Wherever the predicted temperature is less than or equal to some critical value T_0 (typically -1.8°C), the temperature is set to T_0 .

ii. Under climatological ice points (these will usually be determined as being those points where the climatological sea surface temperature is less than or equal to T_0), temperature and salinity at the top model level are set to their climatological values. Surface fluxes of heat and freshwater are set to zero at these points, as is the wind mixing power (used in the mixed layer model).

iii. Convective mixing between adjacent levels is suppressed wherever one of the levels is at a temperature less than or equal to T_0 . This ensures that climatological ice points remain at T_0 at the end of the timestep, and are not changed by convective mixing.

iv. For latitudes at which filtering is performed, steps i and ii are repeated after the filtering.

Appendix B: The Pseudo-Atmospheric Model

For ocean-only runs which include the full ice model, forcing data are required which would normally come from the atmospheric part of the ice model. The 'pseudo-atmospheric' model mimics the atmospheric section by providing the thermodynamic ice model with the forcing fluxes it requires, calculated from climatological forcing data.

The atmospheric ice model usually supplies rates of snowfall and sublimation, S_N and S_B , the net surface heat flux into the leads fraction, F_L , the downward diffusive heat flux through the ice, F_D , and the surface melting heat flux, F_M . In the model, monthly mean climatological snowfall rates and sublimation rates are read in PP format, and made cyclical if cyclic boundary conditions are being used. Where no sublimation data is available a field of zeroes can be included in the initial data. Heat fluxes are calculated by the pseudo-atmospheric model from surface air temperatures and incident solar radiation. At present an air temperature dataset from Schutz and Gates and solar radiation from the 3rd Annual Cycle are being used. The former includes sea ice points, and the latter was derived using prescribed, zonally averaged clouds. Values are therefore of the correct magnitude, if highly zonal in character. 'Pseudo-haney' forcing, and a simple representation of changing albedoes are used to calculate the required heat fluxes from this data.

The albedo used for the leads is the same as that used for the open ocean, namely $\alpha=0.06$. For the ice and snow fractions, the albedo formulation is the same as that used in the CYBER pseudo-atmospheric model, and is different from that used in a fully coupled run. Icy grid boxes are divided into four categories depending on the presence or absence of snow cover, and on whether melting is occurring. Each category has a fixed albedo as follows:

Dry snow	$\alpha=0.8$
Melting snow	$\alpha=0.65$
Dry bare ice	$\alpha=0.7$
Melting bare ice	$\alpha=0.5$

A snow depth of $h_s=0.01\text{m}$ is chosen, somewhat arbitrarily, as the minimum depth of snow to affect albedo. Snow depths less than this are treated as bare ice.

The heat flux into the leads, F_L , is calculated in two parts as is done in the atmospheric model, from the relation

$$F_L = H (T_a - T_F) + (1-\alpha) F_S \quad (\text{B.1})$$

where H is the haney coefficient, currently set to $163.76 \text{ Wm}^{-2}\text{K}^{-1}$, T_a is the surface air temperature in Celsius, and F_S is the incident solar radiation taken from the 3rd Annual Cycle. The first term gives the non-penetrative heat flux, and the second gives the penetrative heat flux over the leads. In this calculation $\alpha=0.06$ as for the ocean model, and the symbols represent the same quantities as in the main body of the text. The leads fraction is assumed to have constant temperature $T_F = -1.8 \text{ }^\circ\text{C}$.

For the ice fraction, equation B.1 becomes

$$F_A = H(T_a - T) + (1-\alpha) F_S \quad (\text{B.2})$$

where T is the surface temperature of the ice or snow, an unknown, and α varies as described in the previous paragraph. The diffusive heat flux, F_D , is given by

$$F_D = \frac{\kappa_I (T - T_F)}{h_E} \quad (\text{3.2})$$

as in the atmospheric part of the full ice model. To solve for T, we assume that the surface temperature, T, is less than zero, so that the frozen snow and ice albedoes apply, and no surface melting occurs. In this case $F_D = F_A$ (neglecting surface heat capacity since there is no diurnal variation in the mean forcing fields) and we can solve for the snow/ice surface temperature T.

$$T = \frac{\gamma T_F + HT_a + F_S(1-\alpha)}{\gamma + H} \quad (\text{B.3})$$

If the value of T obtained from this is less than zero, we have a consistent solution and F_M is set equal to zero. The calculated value of T is then substituted into (3.2) to calculate F_D .

If T obtained above is greater than zero then melting must be occurring, and the albedoes used in its derivation were inappropriate. The result is still valid however, because substituting the (smaller) albedoes appropriate for melting conditions introduces a discontinuity at zero and further increases an already positive temperature. In this case T is assumed equal to zero (the melting point of snow and sea ice) and substituted into equations (B.2) and (3.2) along with the altered albedoes. Values are thus obtained for F_A and F_D (when melting occurs the two are not equal), and the surface melting heat flux, F_M , is then obtained from equation (3.5)

$$F_M = F_A - F_D \quad (\text{3.5})$$

This completes the calculation of heat fluxes required by the thermodynamic ice model. If cyclic boundary conditions are being used all the heat fluxes are made cyclic in the pseudo-atmospheric model before they are passed to the ocean half of the ice model.

Appendix C: Description of Cavitating Fluid Scheme

This appendix describes the details of the cavitating fluid ice dynamics calculations (see Flato and Hibler 1993) as implemented in the unified model. Advection is done using the upwind scheme (on an Arakawa C grid) which is described in Section 4, so what follows is a description of how the ice velocities are derived from dynamic forcing by atmosphere and ocean.

The momentum balance for sea ice, where it is being treated as a continuum, is usually written as

$$\frac{\partial \mathbf{u}}{\partial t} = -mf\mathbf{k} \times \mathbf{u} + \boldsymbol{\tau}_a + \boldsymbol{\tau}_w - mg\nabla H + \mathbf{F} \quad (\text{C.1})$$

where m is the snow and ice mass per unit area, \mathbf{u} is the ice velocity, t is time, f is the coriolis parameter $2\omega \sin\Phi$, \mathbf{k} is the upward unit normal, $\boldsymbol{\tau}_a$ and $\boldsymbol{\tau}_w$ are forces per unit area due to air and water drag respectively, g is the acceleration due to gravity, H is the sea surface dynamic height, and \mathbf{F} is the force per unit area due to variations in internal ice stress. (This equation neglects the non-linear momentum advection term. This term is usually omitted, even from quite complex models, partly because it can be shown to be small in most cases through a scaling analysis, and partly because it is very difficult to handle.) In our model we neglect acceleration (i.e. assume a steady state and diagnose velocities from a balance of the forces) and sea surface tilt because they are small relative to the other terms. Sea surface tilt is also a little hard to define in a rigid lid ocean model. The cavitating fluid approximation allows the internal ice forces, \mathbf{F} , to be expressed as

$$\mathbf{F} = -\nabla P \quad (\text{C.2})$$

where P is the internal ice pressure. (The simplest case is free drift where P is zero everywhere i.e. internal ice forces are neglected and the coriolis force is balanced against the wind and water stress terms.)

In the coupled model, surface wind stress is diagnosed by boundary layer subroutines in the atmosphere model and passed to the ocean model as coupling fields. In ocean only runs it is provided as climatological forcing, thus $\boldsymbol{\tau}_a$ can be taken as given. The water stress, $\boldsymbol{\tau}_w$, is calculated in the model using a quadratic drag law derived by McPhee and described in Flato and Hibler 1992. The vector stress is

$$\boldsymbol{\tau}_w = C_w^* [(\mathbf{U}_w - \mathbf{u}) \cos\psi + \mathbf{k} \times (\mathbf{U}_w - \mathbf{u}) \sin\psi] \quad (\text{C.3})$$

where

$$C_w^* = \rho_w C_w |(\mathbf{U}_w - \mathbf{u})| \quad (\text{C.4})$$

and C_w is the water drag coefficient ($0.0055 \text{ kg m}^{-2} \text{ s}^{-1}$), ρ_w is the density of sea water and Ψ is a constant water turning angle (assumed to be 25° , or -25° in the southern hemisphere). Because this drag coefficient depends on the ice velocity, a double timestep is used in which drag coefficients are calculated using ice velocities from the previous timestep. These are used to calculate a free drift field and correct it, and the drag coefficients are recalculated using these intermediate velocities. The velocity calculations are then repeated with the new drag coefficients to give the final velocity field.

The equation of motion we are solving,

$$-m f\mathbf{k}\times\mathbf{u} + \boldsymbol{\tau}_a + C_w^*[(\mathbf{U}_w-\mathbf{u})\cos\Psi + \mathbf{k}\times\mathbf{u}(\mathbf{U}_w-\mathbf{u})\sin\Psi] = \nabla P \quad (\text{C.5})$$

can be rewritten, with terms involving \mathbf{u} separated out, as

$$-\mathbf{A}\mathbf{u} - \mathbf{B}\mathbf{k}\times\mathbf{u} + \boldsymbol{\tau} = \nabla P \quad (\text{C.6})$$

where $A = C_w^* \cos\Psi$

$B = mf + C_w^* \sin\Psi$

$\mathbf{C} = \boldsymbol{\tau}_a + C_w^* \cos\Psi \mathbf{U}_w + C_w^* \sin\Psi \mathbf{k}\times\mathbf{U}_w$

We want first to solve this equation with P zero everywhere (although we will solve it for arbitrary P so that the same solution can be applied on the second half timestep where the ice pressure has been increased from zero by application of the correction scheme). If we resolve into θ and ϕ coordinates, on a spherical Arakawa B staggered grid i.e.

$$\begin{array}{ccc} h+ & & h+ & & h+ \\ & u>v^{\wedge} & & u>v^{\wedge} & & u>v^{\wedge} \\ h+ & & h+ & & h+ \\ & u>v^{\wedge} & & u>v^{\wedge} & & u>v^{\wedge} \\ h+ & & h+ & & h+ \end{array}$$

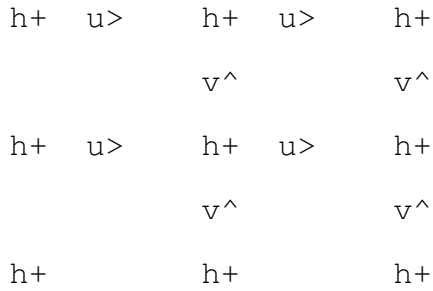
we get

$$\begin{aligned} -Au + Bv + \tau_{\theta} &= \frac{dP}{(r\sin\phi d\theta)} \\ -Av - Bu + \tau_{\phi} &= \frac{dP}{(rd\phi)} \end{aligned} \quad (\text{C.7})$$

This can be rearranged to give an algebraic solution:

$$\begin{aligned} u &= \frac{A\left(\frac{\tau_{\theta}-dP}{r\sin\phi d\theta}\right) + B\left(\frac{\tau_{\phi}-dP}{rd\phi}\right)}{A^2+B^2} \\ v &= \frac{-B\left(\frac{\tau_{\theta}-dP}{r\sin\phi d\theta}\right) + A\left(\frac{\tau_{\phi}-dP}{rd\phi}\right)}{A^2+B^2} \end{aligned} \quad (\text{C.8})$$

Unfortunately this B grid formulation has an alternating grid point instability in the correction scheme, as described in Flato and Hibler 1992, so following them we have implemented the ice model on an Arakawa C grid with u and v components defined at separate points as shown



to eliminate the instability. The drawback with this approach is that an algebraic solution of the free drift equation is no longer possible, because the u and v components are defined at separate points and so cannot be eliminated by adding the component equations. An iterative solution is possible and converges relatively quickly.

Take the equation of motion

$$-A\mathbf{u} - B\mathbf{k} \times \mathbf{u} + \boldsymbol{\tau} = \nabla P \tag{C.6}$$

and resolve it into component equations on a spherical C grid where u is the zonal velocity component, v is the meridional velocity component, subscripts x and y denote coefficients valid at u and v velocity points respectively, $\tau_{\theta x}$ is the zonal component of forcing stress defined at u velocity points, $\tau_{\phi y}$ is the meridional stress component defined at v velocity points, and i and j denote positions on the grid.

$$\begin{aligned}
 -A_x u_x + B_x v_x + \tau_{\theta x} &= \frac{\partial P}{(r \sin \phi \partial \theta)_x} \\
 -A_y v_y - B_y u_y + \tau_{\phi y} &= \frac{\partial P}{(r \partial \phi)_y}
 \end{aligned} \tag{C.9}$$

We expand this to show dependence on surrounding velocity points, assuming that A, B, τ , and ∇P are available at both u and v points by consistent averaging/interpolation.

$$\begin{aligned}
 -A_x u_x(i, j) + 0.25 B_x [v_y(i-1, j) + v_y(i, j) + v_y(i-1, j+1) \\
 + v_y(i, j+1)] &= \frac{\partial P}{(r \sin \phi \partial \theta)_x} - \tau_{\theta x} \\
 -A_y v_y(i, j) + 0.25 B_y [u_x(i, j-1) + u_x(i+1, j-1) + u_x(i, j) \\
 + u_x(i+1, j)] &= \frac{\partial P}{(r \partial \phi)_y} - \tau_{\phi y}
 \end{aligned} \tag{C.10}$$

Separating out terms involving $u_x(i, j)$ and $v_y(i, j)$ from those involving surrounding points we get

$$-A_x u_x(i, j) + 0.25 B_x v_y(i, j) = -0.25 B_x [v_y(i-1, j) + v_y(i-1, j+1) + v_y(i, j+1)] + \frac{\partial P}{(r \sin \phi \partial \theta)_x} - \tau_{\theta x}$$

$$-A_y v_y(i, j) + 0.25 B_y u_x(i, j) = 0.25 B_y [u_x(i+1, j) + u_x(i+1, j-1) + u_x(i, j-1)] + \frac{\partial P}{(r \partial \phi)_x} - \tau_{\phi y} \quad (C.11)$$

For clarity I will substitute

$$R1 = -0.25 B_x [v_y(i-1, j) + v_y(i-1, j+1) + v_y(i, j+1)] + \frac{\partial P}{(r \sin \phi \partial \theta)_x} - \tau_{\theta x}$$

$$R2 = 0.25 B_y [u_x(i, j-1) + u_x(i+1, j-1) + u_x(i+1, j)] + \frac{\partial P}{(r \partial \phi)_y} - \tau_{\phi y}$$

which leaves

$$\begin{aligned} -A_x u_x(i, j) + 0.25 B_x v_x(i, j) &= R1 \\ -A_y v_y(i, j) - 0.25 B_y u_x(i, j) &= R2 \end{aligned} \quad (C.12)$$

where R1 and R2 depend on neighbouring velocity points. These equations can be rearranged and combined to give

$$\begin{aligned} u_x(i, j) &= \frac{-1}{\det(A_x R1 + 0.25 B_x R2)} \\ v_x(i, j) &= \frac{-1}{\det(A_x R2 - 0.25 B_y R1)} \end{aligned} \quad (C.13)$$

where

$$\det = A_x A_y + \frac{1}{16} B_x B_y$$

Although R1 and R2 depend on neighbouring velocities, if this calculation is repeated for each point on the grid several times, starting with the velocity field from the previous timestep, the velocity increments become small and the solution converges.

Once this free drift solution has been obtained, we need to correct the velocity field to allow for the internal forces in the ice - the cavitating fluid scheme. Free drift gives a realistic velocity field but allows excessively thick ice to build up because there is no resistance to convergence. The purpose of the correction scheme is to alter velocity components so as to reduce convergence. Rather than treat the ice as completely incompressible, an ice strength parameterisation is used such that the internal ice pressure is not allowed to exceed a calculated maximum, the ice strength, in each grid box. If this ice strength is reached, some convergence is retained in the grid square as a crude representation of ridging / rafting. The ice strength is given by

$$P_{max} = P^* h \exp[-C(1-A)] \quad (C.14)$$

where P* and C are tunable constants (P*=27.5 kN.m⁻² ; C=20), h is the mean ice depth (NB this does not include snow depth at present), and A is the ice fraction. Each velocity correction increases the internal ice

pressure P , but P is not allowed to exceed P_{max} .

To derive the velocity corrections and pressure increments, start with the equation of motion again.

$$-A \mathbf{u} - B \mathbf{k} \times \mathbf{u} + \boldsymbol{\tau} = \nabla P \quad (\text{C.6})$$

We want corrected fields $\mathbf{u} + \mathbf{u}'$ and $P + P'$ (where ' indicates a correction) such that $P + P' \geq 0$ and

$$\begin{aligned} \nabla \cdot (\mathbf{u} + \mathbf{u}') &\geq 0 & \text{if } P + P' = 0 \\ \nabla \cdot (\mathbf{u} + \mathbf{u}') &= 0 & \text{if } 0 < P + P' < P_{max} \\ \nabla \cdot (\mathbf{u} + \mathbf{u}') &\leq 0 & \text{if } P + P' = P_{max} \end{aligned}$$

These corrected fields will satisfy the same equation of motion, so that

$$-A(\mathbf{u} + \mathbf{u}') - B \mathbf{k} \times (\mathbf{u} + \mathbf{u}') + \boldsymbol{\tau} = \nabla(P + P') \quad (\text{C.15})$$

which can be simplified to give

$$-A(\mathbf{u} + \mathbf{u}') - B \mathbf{k} \times \mathbf{u} + \boldsymbol{\tau} = \nabla(P + P') \quad (\text{C.16})$$

Subtracting (C.6) from (C.16) gives a velocity correction of

$$\mathbf{u}' = \frac{-1}{A} \nabla P' \quad (\text{C.17})$$

so now we require an expression for the pressure correction, P' , such that $\nabla \cdot (\mathbf{u} + \mathbf{u}') = 0$. Substituting gives

$$\begin{aligned} \nabla \cdot (\mathbf{u} - \frac{1}{A} \nabla P') &= 0 \\ \nabla \cdot (\frac{1}{A} \nabla P') &= \nabla \cdot \mathbf{u}' \end{aligned} \quad (\text{C.18})$$

(This Laplacian form is the source of the checkerboard instability in the B grid formulation.)

Hibler solves these for a spherical Arakawa C grid giving divergence

$$\begin{aligned} \nabla \cdot \mathbf{u} &= \frac{1}{r \cos \phi (j + \frac{1}{2})} \left[\frac{1}{\Delta \theta} (u(i+1, j) - u(i, j)) \right. \\ &\quad \left. + \frac{1}{\Delta \phi} (v \cos \phi(i, j+1) - v \cos \phi(i, j)) \right] \end{aligned} \quad (\text{C.19})$$

From this the pressure perturbation can be obtained from

$$P' = \frac{-\nabla \cdot \mathbf{u} r^2 \cos \phi (j + \frac{1}{2})}{\frac{1}{\Delta \theta^2} \left[\frac{1}{A_x(i+1, j)} \cos \phi (j + \frac{1}{2}) + \frac{1}{A_x(i, j)} \cos \phi (j + \frac{1}{2}) \right] + \frac{1}{\Delta \phi^2} \left[\frac{\cos \phi (j+1)}{A_y(i, j+1)} + \frac{\cos \phi (j)}{A_y(i, j)} \right]} \quad \text{C.20}$$

and the corresponding velocity corrections are

$$u'(i,j) = \frac{-1}{(A_x(i,j) \cos\phi(j+\frac{1}{2}))} \frac{P'(i+1,j+1)}{\Delta\theta}$$

$$u'(i+1,j) = \frac{-1}{(A_x(i+1,j) r \cos\phi(j+\frac{1}{2}))} \frac{P'(i+1,j+1)}{\Delta\theta}$$

$$v'(i,j) = \frac{-1}{A_y(i,j) r} \frac{P'(i+1,j+1)}{\Delta\phi}$$

$$v'(i,j+1) = \frac{-1}{A_y(i,j+1) r} \frac{P'(i+1,j+1)}{\Delta\phi}$$

These velocity corrections, if added to the initial field, will ensure that $\nabla \cdot (\mathbf{u}+\mathbf{u}')$ is exactly zero.

The relaxation procedure is as follows. The initial u field is one that satisfies equation (C.6) (i.e. free drift or a modified free drift field with a non-zero pressure field). The entire grid is swept through point by point several times applying velocity corrections and increasing the internal ice pressure by corresponding increments, with the current value equal to the initial value plus all subsequent corrections. This is repeated until the largest correction is smaller than a specified tolerance, with several sweeps of the rows close to the poles required on each pass through the grid to ensure quick convergence on the spherical grid.

At a given grid cell, first the divergence is calculated using the most recent velocity components. If this is greater than zero, and the pressure is zero, nothing further needs to be done. If the divergence is negative, the velocity and pressure fields are corrected, unless the new pressure field would exceed P_{max} , the ice strength, in which case the pressure correction $P'=P_{max}-P$ is applied, with corresponding velocity corrections. This maintains some convergence in the grid square but ensures that P does not exceed P_{max} . If the divergence is positive and the pressure is finite, either P' as calculated above, or $P' = -P$ is applied, whichever is smaller. This ensures either zero divergence and finite pressure, or zero pressure and finite divergence.

Because the acceleration term has been dropped from the equation of motion, a timestep does not appear explicitly in the equation of motion (although it does appear in the advection equations), however the non-linear water drag terms (which appear in the A and B coefficients) are treated by Hibler through a two-step timestepping scheme. We use the same procedure, starting with an initial velocity field u^k from the previous timestep, and an initial pressure field which is zero everywhere. From the initial velocity field we calculate drag coefficients and thus the A and B coefficients and forcing τ . These are then used to calculate free drift velocities on the C grid, with the initial velocity field entered as a 'first guess' for the relaxation scheme. This free drift field then has the cavitating fluid correction scheme applied to it using the same A coefficients until the largest velocity correction on a sweep through the grid is smaller than the specified tolerance, and the first half timestep is complete. At this point the drag coefficients, A and B coefficients, and forcing τ , are recalculated using the intermediate velocities. The free drift calculations are repeated, using the intermediate velocity and pressure fields as the first guess, and these new drag coefficients.

Finally the cavitating fluid corrections are applied for the second time to give the final velocity and pressure fields. This timestepping scheme is shown in compact form in Flato and Hibler 1992, equations 15a and 15b. Since the ocean and atmosphere model fields are defined on the Arakawa B staggered grid, and ice model fields on the C grid, interpolations are required between mass and velocity points, and also between B and C grids, at different stages in the timestepping. In order to do this as consistently as possible and to minimise both interpolations and errors, I decided to follow the atmospheric boundary layer routines in treating drag coefficients etc. First velocities (i.e. currents, ice velocities) are interpolated to mass points, and the velocity magnitudes and hence drag coefficients are calculated. The drag coefficient C_w^* is used to calculate A_x and A_y ($= C_w^* \cos\psi$) and B_x and B_y ($= -mf + C_w^* \cos\psi$) for both u and v velocity points on the C grid.

Once a velocity field has been obtained, it is necessary to advect ice depth, ice fraction and snow depth. Simple upstream differencing is used and the C grid formulation makes this particularly straightforward with no velocity interpolations required. The advection scheme is detailed in Section 4 of the main section of the documentation, as it is shared with the simple ice dynamics scheme. The advective change in ice depth, part of the continuity equation, are given by

$$\frac{\partial h}{\partial t} = -\nabla \cdot (\mathbf{u}h)$$

where h is the mean ice depth. Similar equations hold for ice concentration, A, and grid box mean snow depth ($A.h_s$). And that completes the cavitating fluid dynamic sea ice model formulation.

The ocean model requires the basal stress from the ice portion of grid boxes as input to its dynamic calculations in CLINIC. With all other ice model options, the wind stress is added to the ocean unaltered even if sea ice is present. In coupled and ocean-only runs including cavitating fluid dynamics, the wind stress components are weighted by the leads fraction (interpolated to the UV grid) before being added to the ocean, and by the ice fraction (similarly interpolated) before being passed to the ice dynamics subroutines. This is done in subroutine INIT_OCEAN_ICE. In coupled runs, it may be more consistent to do this in the atmospheric boundary layer routines, but as this would mean two extra coupling fields for probably negligible benefit it has not been implemented.

Wind mixing energy, which is a field on the tracer grid required as input to the mixed layer model, should also have different treatment under sea ice in the cavitating fluid model. Previously this field was zeroed under sea ice, leading to very shallow mixed layers, but in the present 'frozen' coupled model a wind mixing energy based on leads drag coefficients only, and weighted by the leads fraction, is diagnosed in the boundary layer model and passed to the ocean as a coupling field. After consulting Roderick Smith (CR), I intended to treat WME in the following way in coupled experiments. The 'leads' WME, as it is calculated at present in the frozen climate model, was added to a component due to keel stirring etc. under sea ice. The ice contribution to the mixing energy can be derived from the ice-ocean stress τ_w , which is given by equation C.3. The magnitude of the ice-ocean stress is given by

$$\tau_w = \rho_w C_w |\sigma_w - \mathbf{u}|^2$$

and the energy available for mixing is

$$M = \tau_w \cdot (U_w - u)$$

which can be rearranged to give

$$M = \left[\frac{|\tau_w|^3 (\cos \psi)^2}{(\rho_w C_w)} \right]^{\frac{1}{2}}$$

When this mixing energy was calculated from the ice-ocean stress and used by the mixed layer model, it gave unrealistically deep mixed layers under ice. At present (4.0) this part of the model code is inactive, and further work on implementation may be appropriate if the cavitating fluid scheme is developed further.